The Journal of Nutrition
Ingestive Behavior and Neurosciences

Postnatal Iron Deficiency Alters Brain Development in Piglets[1–3]

Brian J Leyshon,[4] Emily C Radlowski,[5] Austin T Mudd,[6] Andrew J Steelman,[4–6] and Rodney W Johnson[4–6]*

[4]Division of Nutritional Sciences, [5]Department of Animal Sciences, and [6]Neuroscience Program, University of Illinois, Urbana, IL

Abstract

Background: Cognitive deficits associated with postnatal iron deficiency (ID) suggest abnormal brain development, but little is known about animals with gyrencephalic brains.

Objective: The objective was to assess the impact of ID on brain development in piglets.

Methods: Male and female Yorkshire piglets were reared from postnatal day (PD) 2 until PD 29 or 30 by using milk replacer adequate [control (CON)] or deficient (100 compared with 10 mg/kg) in iron and subjected to MRI to assess brain macrostructure, microstructure, and metabolites in the dorsal hippocampi and intervening space. After MRI, brains were collected for histology. Hematocrit, hemoglobin, and liver iron were measured to determine iron status.

Results: Hematocrit and hemoglobin in ID piglets were less than CON after PD 14 ($P < 0.001$), and at the study end liver iron in ID piglets was less than CON ($P < 0.001$). Brain region volumes were not affected by ID, but changes in brain composition were evident. ID piglets had less white matter in 78,305 voxels, with large clusters in the hippocampus and cortex. ID piglets had less gray matter in 13,625 voxels primarily in cortical areas and more gray matter in 28,017 voxels, most notably in olfactory bulbs and hippocampus. The major effect of ID on white matter was supported by lower fractional anisotropy values in the corpus callosum (0.300 compared with 0.284, $P = 0.006$) and in whole brain white matter (0.313 compared with 0.307, $P = 0.002$) in ID piglets. In coronal brain sections, corpus callosum width was less ($P = 0.043$) in ID piglets. Inositol was lower ($P = 0.01$) and phosphocholine was higher ($P = 0.03$) in hippocampus of ID piglets.

Conclusions: Postnatal ID in piglets affects brain development, especially white matter. If the effects of ID persist, it might explain the lasting detrimental effects on cognition. *J Nutr* 2016;146:1420–7.

Keywords: iron deficiency, neurodevelopment, white matter, myelin, oligodendrocyte, piglet, neonatal, micronutrient deficiency, magnetic resonance imaging, histology

Introduction

Iron deficiency (ID)[7] is the most common micronutrient deficiency in the world, affecting ~2 billion people in both developing and industrialized nations (1). ID affects all age groups, but children aged 0–5 y are most vulnerable because of the rapid brain growth and development that occurs during the first year of life (2). During this early sensitive period, iron is needed for neurodevelopmental processes, including energy metabolism, neurotransmission, and myelination (2–5). Disrupting neurodevelopment in the neonate can result in cognitive impairment and behavioral problems that endure for many years, if not a lifetime (6). Young adults that experienced ID as infants had poorer executive function, pattern recognition, and spatial memory (7). Furthermore, children at 10 y of age had slower reaction times and impaired inhibitory control if they experienced ID anemia during infancy (8). Early-life ID has been linked to poorer math and writing abilities, increased hesitancy and anxiety, reduced attention and planning ability, increased visual and auditory latencies, reduced language skills, and reduced motor skills (3, 5). Many outcomes related to ID suggest white matter development is vulnerable.

Oligodendrocytes synthesize and maintain myelin in the central nervous system (1) and are the principle cells in the brain that stain for iron under normal conditions (9). Myelination is a metabolically intensive process, and synthesis and maintenance of myelin requires substantial energy turnover by the oligodendrocytes (10). Iron is a key cofactor for production of energy and

[1] Supported by NIH grant HD069899 and National Institute of Environmental Health Sciences grant T32 ES007326 (ECR).
[2] Author disclosures: BJ Leyshon, EC Radlowski, AT Mudd, AJ Steelman, and RW Johnson, no conflicts of interest.
[3] Supplemental Table 1 and Supplemental Figures 1–4 are available from the "Online Supporting Material" link in the online posting of the article and from the same link in the online table of contents at http://jn.nutrition.org.
[7] Abbreviations: CON, control; DTI, diffusion tensor imaging; ID, iron-deficient or iron deficiency; MRS, magnetic resonance spectroscopy; MBP, myelin basic protein; NGS, normal goat serum; PD, postnatal day; TBS, Tris-buffered saline; VBM, voxel-based morphometry.
*To whom correspondence should be addressed. E-mail: rwjohn@illinois.edu.

Manuscript received September 8, 2015. Initial review completed October 25, 2015. Revision accepted April 29, 2016.
First published online June 8, 2016; doi:10.3945/jn.115.223636.

substrates such as FAs needed for myelination (9). Most research in this area has used rodent models. Myelination in the lissencephalic rat and mouse brain occurs postnatally. However, myelination in the gyrencephalic human brain initiates before birth and continues into the postnatal period (11). As such, the effects of postnatal ID on the development of the human brain are not fully understood.

The present study investigated the effects of postnatal ID on brain development in a neonatal piglet model. The piglet has a gyrencephalic brain with similar growth and myelination patterns to humans (12, 13). One study reported poor performance in a hippocampal-dependent spatial T-maze task and lower iron concentration in the hippocampus when piglets were fed an ID diet from postnatal days (PD) 2 to 28 (14). No effects of ID on whole brain and hippocampal volume in piglets were found by MRI (14), but sophisticated tools for assessing brain macrostructure, microstructure, and metabolites in piglets by MRI were not available at the time. Therefore, in the present study we used a newly developed MRI toolset for piglets (15) to assess the impact of ID on gray and white matter volume in discrete brain areas, white matter integrity, and several metabolites indicative of neural and glial health. We report substantial developmental alterations caused by ID.

Methods

Animals, housing, and feeding. A total of 20 naturally farrowed domestic Yorkshire piglets (12 males and 8 females) from 3 litters were obtained from the University of Illinois swine herd and assigned to either the control (CON) diet or the ID diet, controlling for litter of origin, body weight, and sex. Piglets assigned to the CON diet received an intramuscular iron dextran injection (200 mg, Uniferon), shortly after birth (standard swine industry practice to ward off ID). Piglets remained with the sow and littermates for 24–48 h to receive colostrum and then were delivered to the biomedical animal facility. Because sow's milk has a low iron concentration (~1.79 μmol/mL), it was reasoned that intake of colostrum would have minimal effects on piglet iron status (16). Piglets were individually housed in cages as previously described and were provided a toy (plastic jingle ball; Bio-Serv) and towel for environmental enrichment (17). A 12-h light/12-h dark cycle was maintained with light from 0700 to 1900. The piglets were weighed each morning. All animal care and experimental procedures were performed in accordance with the National Research Council Guide for the Care and Use of Laboratory Animals and approved by the University of Illinois at Urbana-Champaign Institutional Animal Care and Use Committee.

Diets. Powdered sow milk replacer diets were formulated at Test Diet to the same specifications used previously (14). Piglets were assigned to either the CON diet (100 mg Fe/kg solids) or ID diet (10 mg Fe/kg solids) controlling for body weight, sex, and litter of origin; besides iron, all diets met the NRC recommended requirements (18). Piglets were fed 4 times/d for a total of 300 mL/kg body weight each day as described previously (14). Piglets consumed their entire meal, although by the end of the study several ID piglets took longer to finish their meals. No extra water was provided.

Iron status assessment. Blood samples were taken from the jugular vein weekly starting at PD 7 and used to assess hematocrit and hemoglobin as described previously (14). The criterion for anemia in swine is hemoglobin <8 g/dL (18). To assess iron reserves at the end of the study (PD 29 or 30), piglets were intracardially perfused with PBS to flush blood from vasculature, 1 g liver tissue was taken, and iron concentration was analyzed in wet tissue via inductively coupled plasma mass spectrometry as previously described (14).

Magnetic resonance imaging. On PD 29 or 30, piglets were anesthetized by use of a telazol:ketamine:xylazine solution [50 mg tiletamine plus 50 mg zolazepam reconstituted with 2.5 mL ketamine (100 g/L) and 2.5 mL xylazine (100 g/L); Fort Dodge Animal Health], and anesthesia was maintained via inhalation of isoflurane (98% oxygen and 2% isoflurane). After the piglet was fully anesthetized, it was restrained to prevent movement and placed in the MRI scanner. An MRI-compatible pulse oximeter was used to monitor piglet vital signs during the MRI procedure.

A Siemens MAGNETOM Trio 3T imager with a 32-channel head coil was used to conduct all MRI. For macrostructural analysis, anatomical data were acquired via a T1-weighted, magnetization-prepared, rapid gradient-echo (T1 MPRAGE) sequence by use of the following parameters: repetition time, T_R = 1900 ms; echo time, T_E = 2.49 ms; inversion time, T_I = 900 ms; flip angle = 9°, and slice thickness = 0.7 mm. A final voxel size of 0.7 mm^3 isotropic was used across the entire head from the snout to the cervical/thoracic spinal cord joint as described previously (12). All methods utilized for brain region volume estimation and voxel-based morphometry (VBM) analysis were performed as

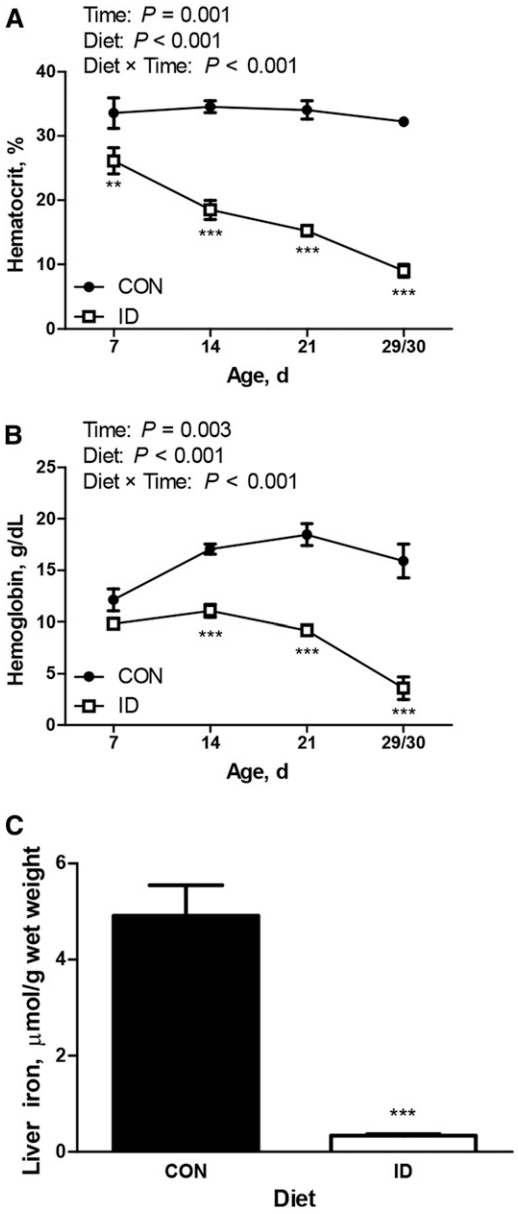

FIGURE 1 Hematocrit (A), hemoglobin concentration (B), and liver iron concentration (C) of piglets fed ID or CON diet from postnatal day 2 through postnatal day 29 or 30. Values are means ± SEMs (n = 3–10 because of missing samples). **,***Different from CON at that time: $^{**}P < 0.01$, $^{***}P < 0.001$. CON, control; ID, iron-deficient.

previously described by Radlowski et al. (19) and Conrad et al. (15, 20). Clusters consisting of <20 edge-connected clusters were not considered for analysis. Corresponding anatomical regions were assigned to voxel clusters of statistically significant difference by use of a digital piglet brain atlas (15). Cortical regions of significant voxel clusters were estimated by use of a brain atlas for adult pigs (21).

Microstructural data were acquired by use of diffusion tensor imaging (DTI) as previously described (22). Briefly, the following parameters were used: repetition time, T_R = 5000 ms; echo time, T_E = 91 ms; averages = 3; diffusion weightings = 2; b value of 1000 s/mm^2. Forty slices 2.00 mm thick were collected utilizing a matrix size of 100 × 100 and a final voxel size of 2.0 mm isotropic throughout the brain. Analysis was performed by use of the diffusion toolbox in the FSL software package as described previously (19).

Brain metabolites were measured via magnetic resonance spectroscopy (MRS) as previously described (19). A single 12 × 25 × 12-mm voxel was placed across the left and right dorsal horns of the hippocampi, including the intervening space consisting of nonhippocampal tissue. A spin echo chemical shift sequence was performed by use of the following parameters: echo time, T_E = 30 ms; repetition time, T_R = 3000; 128 averages; field of view = 200 mm. Water-suppressed and non-water-suppressed data were collected. All MRS data were analyzed by use of the LC Model 6.3 fitting program (19).

Tissue preparation. After MRI, anesthesia was maintained, and piglets were euthanized by intracardial perfusion with PBS (phosphate-buffered saline) followed by perfusion with 4% paraformaldehyde/PBS solution. Brains were removed, weighed, and stored in 4% paraformaldehyde for 2 mo. Following analysis of MRI data, the corpus callosum was selected for further evaluation, and a tissue block containing the posterior half of the corpus callosum and surrounding tissue was dissected from the right hemisphere of each brain. Tissue was sunk in 30% sucrose/PBS solution for cryoprotection. Tissue was then placed in a plastic "boat," coated with optimal cutting temperature medium, and frozen in an acetone bath

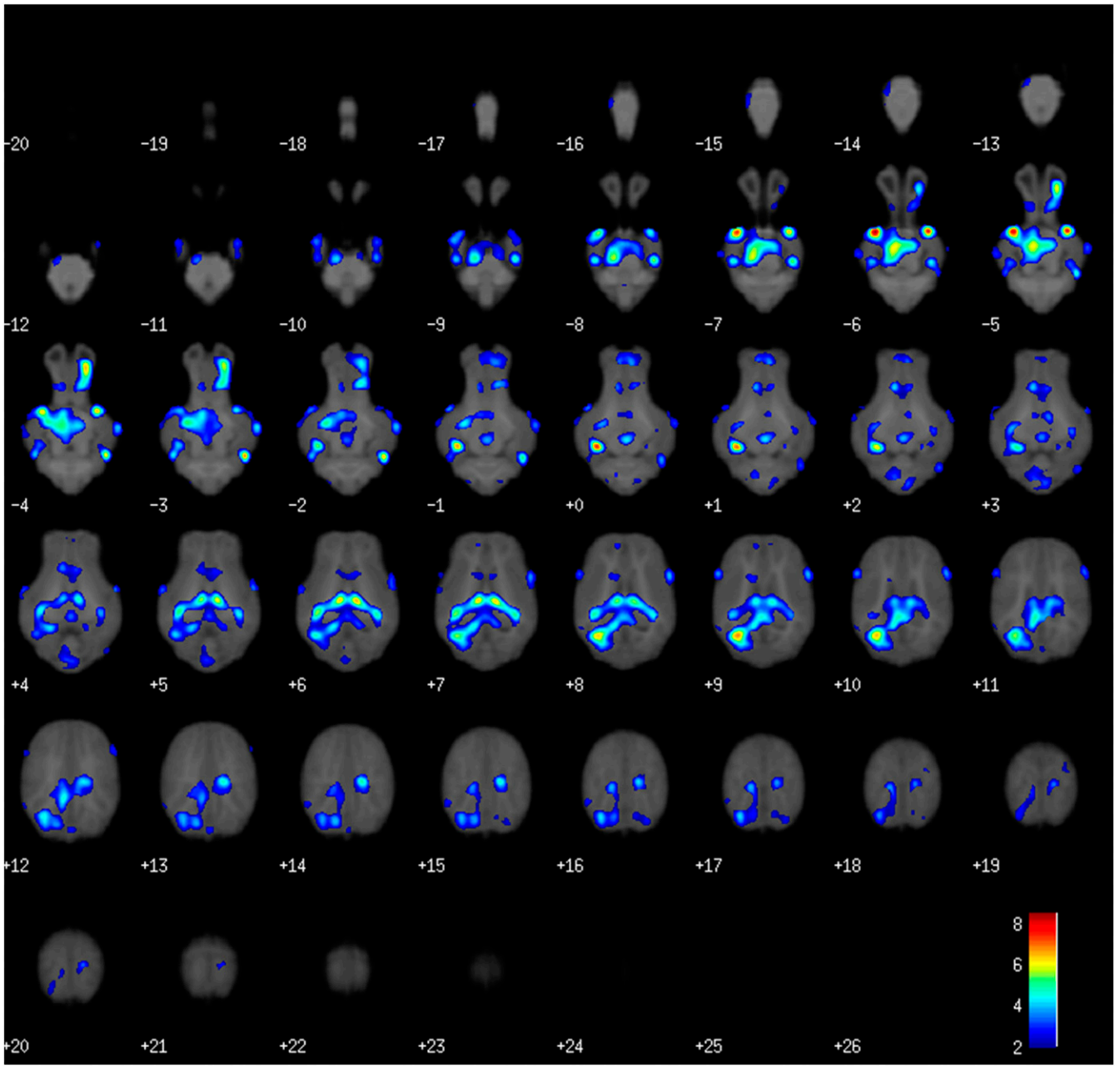

FIGURE 2 Heat map showing brain areas with less white matter in piglets fed iron-deficient diet compared with control diet from postnatal day 2 through postnatal day 29 or 30. The heat map is overlaid on axial piglet brain atlas sections of 1-mm-thick slices. Increasing slice numbers (from − to +) indicate inferior to superior directionality. The color corresponds to the level of significance (pseudo-*t* statistic).

cooled with dry ice. The resulting block was sectioned at 30 μm and stored in cryoprotectant at −20°C until staining.

Immunohistochemical staining. Sections were stained while free-floating. After being initially washed in Tris-buffered saline (TBS), sections were placed in 2× SSC at 70°C for 2 h, rinsed in 2× SSC for 15 min, and then rinsed in TBS. Sections were blocked in 4% normal goat serum (NGS), 0.3% Triton X-100 TBS solution for 1 h at room temperature before being placed in antibody solution [TBS, 3% NGS, 0.3% Triton X-100, 1:1000 rat anti-myelin basic protein (MBP); catalog no. ab7349; Abcam], incubated at 4°C overnight, and rinsed in TBS before incubation in secondary antibody solution [3% NGS, 0.3% Triton X-100, 1:1000 goat anti-rat IgG (Jackson Immunoresearch Laboratories), and 3% NGS] for 1 h. With 10 min remaining in secondary antibody staining period, NucBlue Fixed Cell Stain ReadyProbe reagent (4′,6′-diamino-2-phenylindole stain) was added according to the manufacturer's instructions. Tissue was then washed 3 times in TBS and mounted with ProLong Gold Antifade medium. Tissues were imaged by use of a Zeiss LSM 700 confocal microscope with Imaris imaging software. Per pig, 9 tissue slices were imaged, and 3 *z* stacks were taken in the corpus callosum of each slice, providing 27 *z* stacks/pig for analysis. The *z* stacks were taken beginning when the first slice signal was visible to where the last slice signal was visible. The *z* stacks were then cut in half, and the "top" half (closer to the microscope aperture) was collapsed into a maximum intensity projection. Axiovision software was used to semiautomatically quantify fluorescing area and intensity in

TABLE 1 Brain areas differing in gray or white matter volume between CON and ID piglets as shown by voxel-based morphometry analysis[1]

			Cluster information			Local maxima coordinates		
				FDR-corrected				
Tissue type	Comparison	Anatomic region	Voxels, *n*	*P* value	Pseudo-*t*	*x*	*y*	*z*
White matter	ID < CON	Pyriform cortex	78,024	0.002	8.52	−11	9	−6
		Pyriform cortex	—	0.003	8.01	12	10	−6
		Left hippocampus	—	0.002	7.54	−12	−6	0
		Cerebellum	64	0.037	2.48	1	−15	−8
		Insular cortex	184	0.044	1.38	−8	36	2
		Pons	33	0.047	0.85	7	−8	−16
	ID > CON	No significant differences						
Gray matter	ID < CON	Dorsal posterior cingulate cortex	10,690	0.007	10.9	1	−15	12
		Parahippocampal cortex	—	0.007	9.7	8	−19	7
		Parahippocampal cortex	—	0.007	9.36	−6	−18	8
		Dorsal anterior cingulate cortex	176	0.025	4.89	1	29	9
		Thalamus	224	0.04	4.29	0	8	−1
		Insular cortex	170	0.046	4.02	14	28	9
		Insular cortex	216	0.033	3.91	17	13	14
		Insular cortex	188	0.048	3.82	15	20	10
		Premotor cortex	664	0.033	3.74	1	17	18
		Fusiform gyrus	201	0.04	3.61	17	−9	−2
		Auditory cortex	517	0.007	3.29	−21	1	11
		Insular cortex	554	0.046	2.97	18	16	8
		Insular cortex	—	0.042	2.82	14	27	6
		Amygdala	25	0.04	2.47	−15	10	3
	ID > CON	Right olfactory bulb	11,486	0.009	10.9	6	27	−8
		Left olfactory bulb	—	0.009	10.8	−4	27	−8
		Left olfactory bulb	—	0.016	6.9	5	36	−5
		Left hippocampus	15,262	0.009	7.6	−8	−3	8
		Right hippocampus	—	0.013	6.31	10	−3	7
		Medulla	—	0.026	6.1	0	−25	−18
		Primary visual cortex	100	0.026	3.87	−7	−4	19
		Fusiform gyrus	136	0.046	3.81	13	−12	9
		Perirhinal cortex	116	0.021	3.53	5	−9	9
		Anterior entorhinal cortex	208	0.024	3.17	15	3	−4
		Ventral anterior cingulate cortex	562	0.047	3.13	2	21	8
		Ventral anterior cingulate cortex	—	0.043	2.77	3	12	13
		Insular cortex	—	0.048	0.94	10	16	13
		Perirhinal cortex	59	0.024	2.98	−5	−10	8
		Premotor cortex	60	0.033	2.66	−4	5	19
		Primary visual cortex	28	0.33	2.66	6	1	20

[1] Data from nonparametric permutation tests presented as *n* voxels, FDR-corrected *P* value, and pseudo-*t* value with a threshold at $P < 0.05$ FDR corrected and a minimum cluster size of 20 voxels are shown. The analysis is based on 10 piglets for each treatment ($n = 10$). The comparison column lists the directionality of comparison, i.e., the first set of comparisons describes areas in which ID piglet brains had less white matter than CON brains. Cluster size denotes the number of voxels composing an area of significant difference. Effects of ID were widespread, often resulting in multiple overlapping clusters of voxels that read as a single combined cluster volume. In such instances the volume of the cluster is displayed once with other significant centers in the cluster listed with a minus sign. Local maxima coordinates correspond to a digital piglet brain atlas used for analysis (15). CON, control; FDR, false discovery rate; ID, iron-deficient.

each image, with the base threshold set from the highest image in the dataset and applied to all images. To demonstrate antibody specificity, Western blotting was done by use of the MBP antibody with purified porcine MBP purchased from Sigma (catalog no. SRP5204) and porcine brain protein lysates. The purified porcine MBP from Sigma contained only the 21.5-kDa MBP isotype. Western blotting revealed 3 bands with molecular weights between 17 and 23 kDa, in porcine brain lysates, one of which corresponds to the single band seen in the column loaded with 2 μg of purified MBP with the predicted molecular weight. The other bands present in the porcine brain lysate column are consistent with the 4 forms of MBP present in the pig central nervous system (**Supplemental Figure 1**). No other bands were visible in porcine brain lysates. When lower amounts of purified MBP were loaded, no bands were visible.

Black-Gold staining. Black-Gold II staining was used to detect myelin and performed according to kit instructions (Millipore). Tissue slices 30 microns thick were mounted on slides and dried. Tissue was rehydrated for 2 min in MilliQ water and placed in 0.3% Black-Gold II solution preheated to 60°C. After incubation for 12 min, slides were checked for sufficient staining and returned to Black-Gold II solution for 2-min intervals if needed. Slides were rinsed in MilliQ water and fixed in 1% sodium thiosulfate for 3 min at 60°C, rinsed in MilliQ water, dehydrated in graded ethanol solutions, and mounted. Slides were visualized by use of the Hamamatsu Nanozoomer digital pathology system to capture a single layer at 40×. Hamamatsu NDP.view2 software was used for analysis and quantification of tissue. Measurements of the corpus callosum were taken in reference to the ventral anterior cingulate cortex as a landmark.

Statistical analysis. Sex did not affect body weight or iron status, so data from males and females were pooled by treatment for final analysis. Body weight was analyzed via a 2-factor (treatment × time) repeated-measures ANOVA with Bonferroni post hoc tests by use of GraphPad Prism 5. Hemoglobin and hematocrit were analyzed by use of the MIXED procedure of the SAS software package (SAS Institute). Liver iron concentration, gross brain region volumes, DTI, MRS, immunohistochemistry, and Black-Gold II data were analyzed by use of a 2-sided *t* test within GraphPad Prism 5. Significance was accepted at $\alpha = 0.05$. Data are presented as means ± SEMs.

VBM statistical analysis was performed by use of a *t* test comparing ID and CON groups with no covariates and a false discovery rate (FDR)-corrected α of 0.05 instead of an uncorrected α of 0.01 in order to provide more rigorous statistical validation. The statistical nonparametric methods toolbox was used for VBM analysis (23). Global normalization was performed with an ANCOVA. Pseudo-*t* statistic maps were generated to visualize regional differences in gray or white matter volume between ID and CON groups. To consider a cluster significant, a threshold of ≥20 contiguous voxels was set.

Ten piglets per treatment group were studied. For some measurements, *n* was <10 because of missing blood samples or motion artifacts during MRI. For histology, a subgroup from each treatment was selected for analysis ($n = 6$–7).

Results

Body weight and iron status. Piglet body weight was affected by time ($P < 0.001$) and a diet × time interaction ($P < 0.001$) with ID piglets weighing 0.68 and 1.02 kg less than CON piglets on PDs 27 ($P < 0.05$) and 28 ($P < 0.001$), respectively (**Supplemental Figure 2**). Piglet hematocrit was affected by diet ($P < 0.001$), time ($P < 0.001$), and a diet × time interaction ($P < 0.001$). Hematocrit in ID piglets decreased during the study and was lower than CON on PD 7 ($P = 0.002$), 14, 21, and at the end of study (PD29 or 30; $P < 0.001$; **Figure 1**A). Piglet blood hemoglobin was affected by diet ($P < 0.001$), time ($P = 0.003$), and a diet × time interaction ($P < 0.001$). Blood hemoglobin in ID piglets was lower than CON on PDs 14 and 21 and the end of the study ($P < 0.001$); Figure 1B). At the end of the study, liver iron concentration was markedly lower in piglets provided the ID diet ($P < 0.001$; Figure 1C). Collectively, these data show that iron status was significantly and progressively reduced by the ID diet.

Magnetic resonance imaging. Brain region volumes did not differ between ID and CON piglets as measured by MRI (**Supplemental Table 1**), nor did brain weights taken immediately after death (data not shown). VBM, however, revealed widespread changes in brain composition. **Figure 2** uses a color scale on piglet brain atlas images to highlight all brain areas in which ID piglets had significantly less white matter than did CON piglets ($P < 0.05$ FDR). Areas of greatest difference are shown in red, and lesser but still significant areas are shown in blue. Areas with less white matter in ID piglets map to 6 distinct centers (**Table 1**). A large cluster of 78,024 voxels representing reduced white matter extended through much of the central portion of the brain, with centers of high significance in the left cortex, right cortex, and left hippocampus. Additionally, clusters of voxels with less white matter volume were found in the cerebellum and left insular cortex of ID piglets. There were no brain areas with more white matter in ID piglets than in CON.

Iron deficiency also resulted in alterations in gray matter volume compared with CON piglets, with 14 distinct centers with less gray matter as determined by VBM (Table 1). Gray matter volume was less primarily in the occipital lobe, with smaller clusters of voxels with less gray matter volume in the prefrontal cortex, thalamus, and areas of the cortex (Table 1, **Supplemental Figure 3**). There were 16 centers with more gray matter (Table 1, **Supplemental Figure 4**), with the primary areas of difference located in the olfactory bulbs and hippocampus (**Figure 3**). Of the total voxels affected by ID, 65% represented less white matter, 12% represented less gray matter, and 23% signified more gray matter. Collectively, these data indicate ID preferentially reduced white matter.

White matter tract development was evaluated by DTI. Globally, fractional anisotropy, a marker of white matter microstructural integrity and health, was lower in the white matter of ID piglets than in that of CON piglets ($P = 0.002$; **Figure 4**). Corpus callosum fractional anisotropy was lower in ID piglets than in CON piglets ($P = 0.006$; Figure 4). Consistent with reduced fractional anisotropy values, radial diffusivity, the sum of the 2 minor eigenvectors of diffusion, was higher in the left hippocampus ($P < 0.001$), right hippocampus ($P = 0.01$), and thalamus of ID piglets ($P = 0.003$; **Figure 5**A); no other brain regions differed significantly in radial diffusivity. Mean diffusivity

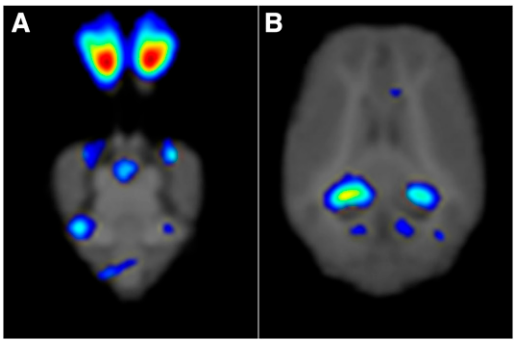

FIGURE 3 Heat map showing higher gray matter in olfactory bulbs (A) and hippocampus (B) of piglets fed the iron-deficient diet than in those fed the control diet from postnatal day 2 through postnatal day 29 or 30. The color corresponds to the level of significance (pseudo-*t* statistic).

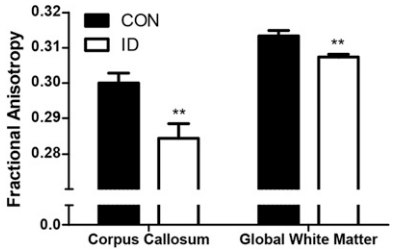

FIGURE 4 Fractional anisotropy of corpus callosum and global white matter in piglets fed the ID or CON diet from postnatal day 2 through postnatal day 29 or 30. Values are means ± SEMs, n = 9–10. **Different from CON for that brain region, $P < 0.01$. CON, control; ID, iron-deficient.

TABLE 2 Comparison of dorsal hippocampal metabolites between CON and ID piglets via magnetic resonance spectroscopy[1]

Metabolite	CON	ID	P value	Functional importance
Glu	5.22 ± 0.14	5.34 ± 0.23	0.68	Excitatory neurotransmitter
PCh	1.49 ± 0.03	1.62 ± 0.03	0.03	Cell membrane/myelin marker
Inositol	9.14 ± 0.26	8.18 ± 0.21	0.01	Glial cell marker, osmolyte
NAA	4.93 ± 0.14	4.89 ± 0.09	0.80	Neuronal marker
Cr + PCr	4.05 ± 0.06	3.88 ± 0.08	0.12	Metabolic activity

[1] Data are presented in absolute units as means ± SEMs, n = 9–10. Phosphocholine was increased in ID hippocampi compared with controls, whereas inositol was reduced. CON, control; Cr, creatine; Glu, glutamate; ID, iron-deficient; NAA, *N*-acetylaspartic acid; PCh, phosphocholine; PCr, phosphocreatine.

values were greater in the left hippocampus ($P < 0.001$), right hippocampus ($P = 0.009$), and thalamus ($P = 0.002$; Figure 5B) in ID piglets than in CON piglets; no other brain regions differed significantly in mean diffusivity. Axial diffusivity, the major eigenvector of water diffusion, was higher in left hippocampus ($P < 0.001$), right hippocampus ($P = 0.011$), and thalamus ($P = 0.004$; Figure 5C) of ID piglets; no other brain regions differed significantly in axial diffusivity. These data further highlight the detrimental effects of ID on white matter development and integrity.

Absolute metabolite concentrations in the dorsal horns of the hippocampi and intervening space were analyzed via MRS (**Table 2**). Phosphocholine was significantly higher in ID piglets than in CON piglets ($P = 0.035$). Inositol, an osmolyte and astrocyte marker, was significantly lower in ID piglets than in CON piglets ($P = 0.01$). Glutamate, *N*-acetylaspartate, creatine, and phosphocreatine did not differ significantly between the 2 groups.

Histology. Immunohistochemistry was used to evaluate MBP content in the corpus callosum. Mean intensity, total intensity, and total area were evaluated; no significant differences were found between the 2 groups (data not shown). Based on findings from the MRI data, the corpus callosum was selected for further histological analysis. To assess the thickness of the corpus callosum, sections were stained with Black-Gold II (**Figure 6**A). Consistent with less white matter, the thickness of the corpus callosum was lower in ID piglets than in CON piglets ($P = 0.043$; Figure 6B). No differences were found in mean intensity between the 2 groups (data not shown).

Discussion

The present study evaluated the effects of ID on neurodevelopment by use of MRI and histology. Clinical criteria for anemia in swine including hematocrit and hemoglobin were reached by the end of the study (18) and were consistent with previous studies (14). VBM demonstrated that ID caused widespread reduction in white matter volume. ID also altered gray matter development, resulting in areas with both more and less gray matter volume compared with CON, a logical outcome because no significant difference in overall brain volume was observed. Thus, similar to what was reported previously by use of MRI with piglets (14), brain development in terms of overall volume or weight is at least partially protected during ID. However, the more detailed data provided by the VBM toolset found brain composition to be profoundly altered. Additionally, DTI revealed lower fractional anisotropy, the gold standard for assessing myelin integrity and health, in both the corpus callosum and globally across white matter in ID piglets. Together, these findings show ID alters brain composition and white matter development.

Notably, hippocampal white matter volume was less in ID piglets, which may play a role in the impaired learning and memory observed with this model (14). In the study by Rytych et al. (14), no difference was found in hippocampal volume between ID piglets and CON. However, VBM for piglets was not available at that time. Using the VBM tool newly adapted to the piglet (15), we were able to detect large changes in white matter and gray matter across several brain regions including the hippocampus. One limitation of this study was the reporting ability of the Statistical nonParametric Mapping toolbox (http://warwick.ac.uk/snpm). Because areas with less white matter were widespread and overlapping, the ability to resolve specific brain areas within a cluster with the Statistical nonParametric Mapping toolbox was limited. For example, a large single cluster of 78,024 voxels with less white matter volume encompassed several brain areas (Table 1). Manual inspection shows that the cluster encompasses portions of the internal capsule, hippocampus, fornix, thalamus, and midbrain. Early-life ID is associated with reduced display of emotions and increased anxiety, which may be affected by alterations in white matter development in these areas (24). Gray matter was lower primarily in the occipital lobe, indicating that visual cortex development may be affected by ID.

One of the primary functions of the thalamus is to act as a "switchboard" for incoming sensory information and the appropriate cortices. The lower thalamic white matter (Figure 2), in context with the aforementioned lower white matter fractional anisotropy, may play a role in the increased visual and auditory latencies seen in children that have experienced early-life ID (25). ID reduced fractional anisotropy in the corpus callosum, the largest white matter structure in the brain, which may contribute to impaired interhemispheric communication. Importantly, impairment of the corpus callosum microstructure correlates with decreased cognitive function (26). Although the thalamus and hippocampi of ID piglets did not significantly differ from CON piglets in terms of fractional anisotropy, radial diffusivity, a measure of the minor diffusion eigenvectors, was greater in ID piglet hippocampi. Greater radial diffusivity is associated with reduced myelination, which allows increased diffusion perpendicular to the primary direction of flow—in this case, the axon. Mean diffusivity, a measure of total diffusivity, was also greater, suggesting less structural organization or cellularity in the ID hippocampus and thalamus. Alternatively, early ID in the piglet may result in greater diffusivity because of

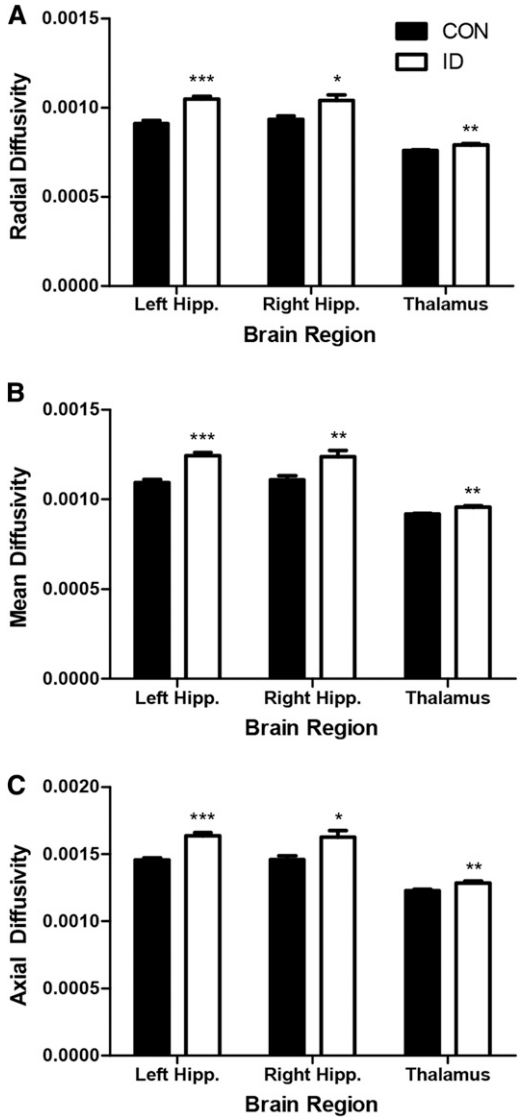

FIGURE 5 Radial diffusivity (A), mean diffusivity (B), and axial diffusivity (C) of the left hippocampus, right hippocampus, and thalamus of piglets fed ID or CON diet from postnatal day 2 through postnatal day 29 or 30. Values are means ± SEMs, $n = 9$–10. *,**,***Different from CON for a given brain region: *$P < 0.05$, **$P < 0.01$, ***$P < 0.001$. CON, control; Hipp., hippocampus; ID, iron-deficient.

reduced dendritic arborization in the hippocampus similar to findings by Jorgenson et al. using the rat model (27).

Inositol and phosphocholine were significantly altered by ID. Inositol is an osmolyte and is also used as an astrocyte marker. That it was lower may indicate decreased astrocyte activity in the hippocampus because of ID. Higher phosphocholine in ID piglets may indicate altered myelination patterns, because phosphocholine readings are increased in cases of myelin damage (28).

After MRI, brain tissue was collected and preserved, allowing MRI data to be compared with histology. This approach is potentially important for interpreting MRI data from human infants that experience ID. After analysis, no differences were found by immunohistochemistry evaluation of corpus callosum MBP. Based on the MRI data, we expected to find reduced MBP staining in the corpus callosum. It is possible that reduced myelination resulted in increased exposure of the MBP epitope and thus confounded the results. Following this observation, the histological myelin stain Black-Gold II was utilized for a larger-scale examination of myelination in the brain. The width of the corpus callosum was found to be lower in ID piglets, further supporting DTI findings that corpus callosum development is altered by postnatal ID. It must be considered that the gross volume of the corpus callosum was not found to differ between the 2 treatments via MRI. However, these measurements were taken under 2 different conditions: one in vivo and one ex vivo, following fixation, freezing, adherence to a slide, and dehydration. This emphasizes the importance of using multiple approaches for quantification when possible.

Although the present study did not go beyond PD 30 or involve an iron repletion phase, a recent study using a similar piglet model reported long-lasting cognitive deficits caused by early postnatal ID (29). Several studies in rodents provide insight into the underlying mechanisms. For example, Felt et al. (30) found rats that were ID anemic as pups exhibited impaired performance in both striatal- and hippocampal-centered tasks as adults, even after normalization of iron status. Others showed ID in the prenatal period affected axonal maturation and dendritic complexity in the adult hippocampus (31). Iron is a cofactor for neurotransmitter synthesis, and early-life ID resulted in altered monoamine metabolism and dopamine receptor (D_2) density in rats (32, 33). Furthermore, rats that experienced early-life ID had less subcortical myelination, despite being fed an iron-sufficient diet after weaning (34). Altered neuronal structure, myelination, and changes in neurotransmitter tone may contribute to acute (14) and chronic (29) behavioral deficits observed in piglets exposed to ID, but this has not been investigated.

The markedly higher gray matter volume in the olfactory bulb of ID piglets was an unexpected finding, although there is some evidence that metals may interact with olfaction. A study of professional welders determined that occupational metal exposure is associated with olfactory dysfunction (35). Further, rats fed an ID diet after weaning displayed altered olfactory behavior, including

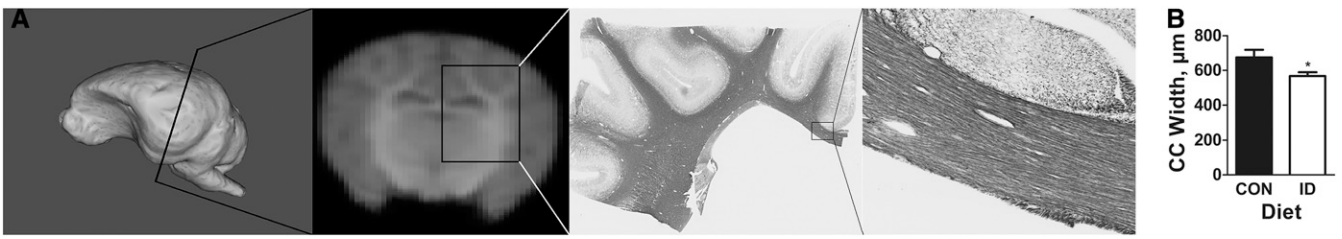

FIGURE 6 Width of CC in piglets fed ID or CON diet from postnatal day 2 through postnatal day 29 or 30. (A) Three-dimensional rendering of piglet brain, MRI coronal section, and tissue sections stained with Black-Gold highlighting where the thickness of the CC was assessed by histology. (B) Comparison of CC width in piglets fed the 2 diets. Values are means ± SEMs, $n = 6$–7. *Different from CON: $P < 0.05$. CC, corpus callosum; CON, control; ID, iron-deficient.

prolonged exploratory time toward attractive odorants compared with controls (36). Further studies in piglets are warranted given the dramatic effects of ID on the olfactory bulb tissue composition and the importance of olfaction to pig behavior.

The current study in neonatal piglets modeled alterations in brain development caused by early-life ID from birth to 4–6 mo of age in the human infant (12). Because the piglet is born with low iron and quickly becomes deficient unless supplemented, this models the situation wherein an infant is born with reduced iron stores and becomes deficient in the ensuing months of early childhood, a pressing concern, because the human infant is unable to effectively regulate iron absorption until ~9 mo of age (37). These results in the piglet suggest brain development, particularly white matter development, is profoundly altered by ID. More research is needed to develop effective therapies for iron repletion and recuperation of developmental losses.

Acknowledgments

BJL and RWJ designed the research and wrote the paper; BJL conducted the research; ATM and AJS provided important assistance with MRI data processing and histology, respectively; BJL and ECR analyzed the data; and RWJ had primary responsibility for the final content. All authors read and approved the final manuscript.

References

1. Fretham SJ, Carlson ES, Georgieff MK. The role of iron in learning and memory. Adv Nutr 2011;2:112–21.
2. Radlowski EC, Johnson RW. Perinatal iron deficiency and neurocognitive development. Front Hum Neurosci 2013;7:585.
3. Georgieff MK. Long-term brain and behavioral consequences of early iron deficiency. Nutr Rev 2011;69(Suppl 1):S43–8.
4. Knickmeyer RC, Gouttard S, Kang C, Evans D, Wilber K, Smith JK, Hamer RM, Lin W, Gerig G, Gilmore JH. A structural MRI study of human brain development from birth to 2 years. J Neurosci 2008;28:12176–82.
5. Lozoff B, Beard J, Connor J, Felt B, Georgieff M, Schallert T. Long-lasting neural and behavioral effects of iron deficiency in infancy. Nutr Rev 2006;64:S34–43.
6. Lozoff B, Jimenez E, Hagen J, Mollen E, Wolf AW. Poorer behavioral and developmental outcome more than 10 years after treatment for iron deficiency in infancy. Pediatrics 2000;105:E51.
7. Lukowski AF, Koss M, Burden MJ, Jonides J, Nelson CA, Kaciroti N, Jimenez E, Lozoff B. Iron deficiency in infancy and neurocognitive functioning at 19 years: evidence of long-term deficits in executive function and recognition memory. Nutr Neurosci 2010;13:54–70.
8. Algarín C, Nelson CA, Peirano P, Westerlund A, Reyes S, Lozoff B. Iron-deficiency anemia in infancy and poorer cognitive inhibitory control at age 10 years. Dev Med Child Neurol 2013;55:453–8.
9. Todorich B, Pasquini JM, Garcia CI, Paez PM, Connor JR. Oligodendrocytes and myelination: the role of iron. Glia 2009;57:467–78.
10. Hirrlinger J, Nave K-A. Adapting brain metabolism to myelination and long-range signal transduction. Glia 2014;62:1749–61.
11. Lenroot RK, Giedd JN. Brain development in children and adolescents: insights from anatomical magnetic resonance imaging. Neurosci Biobehav Rev 2006;30:718–29.
12. Conrad MS, Dilger RN, Johnson RW. Brain growth of the domestic pig (*Sus scrofa*) from 2 to 24 weeks of age: a longitudinal MRI study. Dev Neurosci 2012;34:291–8.
13. Conrad MS, Johnson RW. The domestic piglet: an important model for investigating the neurodevelopmental consequences of early life insults. Annu Rev Anim Biosci 2015;3:245–64.
14. Rytych JL, Elmore MR, Burton MD, Conrad MS, Donovan SM, Dilger RN, Johnson RW. Early life iron deficiency impairs spatial cognition in neonatal piglets. J Nutr 2012;142:2050–6.
15. Conrad MS, Sutton BP, Dilger RN, Johnson RW. An in vivo three-dimensional magnetic resonance imaging-based averaged brain collection of the neonatal piglet (*Sus scrofa*). PLoS One 2014;9:e107650.
16. Miller ER, Ullrey DE. The pig as a model for human nutrition. Annu Rev Nutr 1987;7:361–82.
17. Elmore MR, Burton MD, Conrad MS, Rytych JL, Van Alstine WG, Johnson RW. Respiratory viral infection in neonatal piglets causes marked microglia activation in the hippocampus and deficits in spatial learning. J Neurosci 2014;34:2120–9.
18. Council NR. Nutrient requirements of swine. 10th rev. ed. Washington (DC): The National Academies Press; 1998.
19. Radlowski EC, Conrad MS, Lezmi S, Dilger RN, Sutton B, Larsen R, Johnson RW. A neonatal piglet model for investigating brain and cognitive development in small for gestational age human infants. PLoS One 2014;9:e91951.
20. Conrad MS, Sutton BP, Larsen R, Van Alstine WG, Johnson RW. Early postnatal respiratory viral infection induces structural and neurochemical changes in the neonatal piglet brain. Brain Behav Immun 2015;48:326–35.
21. Saikali S, Meurice P, Sauleau P, Eliat PA, Bellaud P, Randuineau G, Verin M, Malbert CH. A three-dimensional digital segmented and deformable brain atlas of the domestic pig. J Neurosci Methods 2010;192:102–9.
22. Mudd AT, Getty CM, Sutton BP, Dilger RN. Perinatal choline deficiency delays brain development and alters metabolite concentrations in the young pig. Nutr Neurosci 2015 Jun 5 (Epub ahead of print; DOI: 10.1179/1476830515Y.0000000031).
23. Nichols TE, Holmes AP. Nonparametric permutation tests for functional neuroimaging: a primer with examples. Hum Brain Mapp 2002;15:1–25.
24. Chang S, Wang L, Wang Y, Brouwer ID, Kok FJ, Lozoff B, Chen C. Iron-deficiency anemia in infancy and social emotional development in preschool-aged Chinese children. Pediatrics 2011;127:e927–33.
25. Roncagliolo M, Garrido M, Walter T, Peirano P, Lozoff B. Evidence of altered central nervous system development in infants with iron deficiency anemia at 6 mo: delayed maturation of auditory brainstem responses. Am J Clin Nutr 1998;68:683–90.
26. Llufriu S, Blanco Y, Martinez-Heras E, Casanova-Molla J, Gabilondo I, Sepulveda M, Falcon C, Berenguer J, Bargallo N, Villoslada P, et al. Influence of corpus callosum damage on cognition and physical disability in multiple sclerosis: a multimodal study. PLoS One 2012;7:e37167.
27. Jorgenson LA, Wobken JD, Georgieff MK. Perinatal iron deficiency alters apical dendritic growth in hippocampal CA1 pyramidal neurons. Dev Neurosci 2003;25:412–20.
28. Matthews PM, Francis G, Antel J, Arnold DL. Proton magnetic resonance spectroscopy for metabolic characterization of plaques in multiple sclerosis. Neurology 1991;41:1251–6.
29. Antonides A, Schoonderwoerd AC, Scholz G, Berg BM, Nordquist RE, van der Staay FJ. Pre-weaning dietary iron deficiency impairs spatial learning and memory in the cognitive holeboard task in piglets. Front Behav Neurosci 2015;9:291.
30. Felt BT, Beard JL, Schallert T, Shao J, Aldridge JW, Connor JR, Georgieff MK, Lozoff B. Persistent neurochemical and behavioral abnormalities in adulthood despite early iron supplementation for perinatal iron deficiency anemia in rats. Behav Brain Res 2006;171:261–70.
31. Greminger AR, Lee DL, Shrager P, Mayer-Proschel M. Gestational iron deficiency differentially alters the structure and function of white and gray matter brain regions of developing rats. J Nutr 2014;144:1058–66.
32. Jenner P. Brain iron: neurochemical and behavioural aspects. (Topics in Neurochemistry and Neuropharmacology Vol 2). J Neurol Neurosurg Psychiatry 1989;52:293.
33. Beard JL, Felt B, Schallert T, Burhans M, Connor JR, Georgieff MK. Moderate iron deficiency in infancy: biology and behavior in young rats. Behav Brain Res 2006;170:224–32.
34. Wu LL, Zhang L, Shao J, Qin YF, Yang RW, Zhao ZY. Effect of perinatal iron deficiency on myelination and associated behaviors in rat pups. Behav Brain Res 2008;188:263–70.
35. Antunes MB, Bowler R, Doty RL. San Francisco/Oakland Bay Bridge Welder Study: olfactory function. Neurology 2007;69:1278–84.
36. Kumara VMR, Wessling-Resnick M. Influence of iron deficiency on olfactory behavior in weanling rats. J Behav Brain Sci 2012;2:4.
37. Domellöf M, Lönnerdal B, Abrams SA, Hernell O. Iron absorption in breast-fed infants: effects of age, iron status, iron supplements, and complementary foods. Am J Clin Nutr 2002;76:198–204.